The Illumination of Thunderclouds by Lightning:

Part 2: The Effect of GLM Instrument Threshold on Detection and Clustering

Michael Peterson[1], Tracy E. L. Light[1], Douglas Mach[2]

[1] ISR-2, Los Alamos National Laboratory, Los Alamos, New Mexico

[2]Science and Technology Institute, Universities Space Research Association, Huntsville, AL, USA

Corresponding author: Michael Peterson (mpeterson@lanl.gov), B241, P.O. Box 1663 Los Alamos, NM, 87545

Key Points:

- GLM sensitivity is determined by the local threshold at each instrument pixel, which varies across the imaging array and over time
- High thresholds prevent detection of faint illumination, which limits the resolvable detail of flashes or might prevent detection entirely
- Instrument threshold affects all GLM products from event detections to flash clustering and gridded product generation

LA-UR-21-22572

Abstract

Lightning is measured from space using optical instruments that detect transient changes in the illumination of the cloud top. How much of the flash (if any) is recorded by the instrument depends on the instrument detection threshold. NOAA's Geostationary Lightning Mapper (GLM) employs a dynamic threshold that varies across the imaging array and changes over time. This causes flashes in certain regions and at night to be recorded in greater detail than other flashes, and threshold inconsistencies will impose biases on all levels of GLM data products.

In this study, we quantify the impact of the varying GLM threshold on event / group detection, flash clustering, and gridded product generation by imposing artificial thresholds on the event data taken from a thunderstorm with a low instrument threshold (~0.7 fJ). We find that even modest increases in threshold severely impact event (60% loss by 2 fJ, 90% loss by 10 fJ) and group (25% loss by 2 fJ, 81% loss by 10 fJ) detection by suppressing faint illumination of the cloud-top from weak sources and scattering. Flash detection is impacted less by threshold increases (4% loss by 2 fJ), but reductions are still significant at higher thresholds (35% loss by 10 fJ, or 44% if single-group flashes are removed). Undetected pulses cause individual flashes to be split and severely impact the construction of gridded products. All these factors complicate the interpretation of GLM data, particularly when trended over time under a changing threshold.

Plain Language Summary

Lightning is measured from space by optical instruments like the Geostationary Lightning Mapper (GLM). GLM detects rapid changes in cloud brightness from lightning illumination. How much of this illumination can be captured depends on the sensitivity of the instrument, which, for GLM, changes over space and time according to the local instrument threshold. At a low threshold - like we see at night or near the center of the GLM Field of View - flashes can be measured with a tremendous amount of detail. However, when the threshold is high – as it is during the day or in certain places like Colorado – only the brightest portions of a flash might be seen, if the flash is detected at all.

In this study, we characterize the effect of the GLM instrument threshold on each type of GLM data. We find that removing faint detections by imposing higher thresholds affects every type of GLM data. These results demonstrate that situational context is important for evaluating GLM data – particularly when trended over time under a changing threshold.

1 Introduction

Cloud-to-Ground (CG) strokes detected by optical or Radio Frequency (RF) sensors are only a small part of the larger lightning "tree" that extends throughout the cloud. Lightning activity includes a variety of CG and in-cloud phenomena that radiate across a vast range of energies and frequencies. What parts of the flash that are resolved depends on the sensitivity of the instrument and the portion of the electromagnetic spectrum it measures. Both VHF-band Radio Frequency (RF) instruments and optical sensors are capable of mapping major portions of the lightning tree (Rison et al., 1999; Peterson et al., 2018) and detecting powerful emissions from strokes (Light et al., 2001a; Koshak, 2010). RF or optical sensors with low sensitivities may only detect the particularly-energetic strokes or similarly-powerful in-cloud events (Jacobson and Light, 2011), while the most sensitive instruments will be able to map nearly the full extent of the lightning tree – which can cover hundreds of kilometers (Lang et al., 2017; Peterson et al., 2020).

Optical sensors have the additional issue that the lightning emissions – regardless of power – will be significantly modified by absorption and scattering in the cloud medium between the source and satellite (Thomson and Krider, 1982; Koshak et al., 1994; Light et al., 2001b; Brunner and Bitzer, 2020; Peterson, 2020a). Cloud regions that are particularly opaque to lightning signals (either from large optical depths or a composition / geometry that favors diffuse reflection off cloud sides over transmission through the medium) can prevent the detection of even powerful optical lightning signals from space – which we can be seen as anomalies in the radiance data (Peterson, 2020b). Opaque clouds lead to poor Detection Efficiencies (DEs) for instruments like the Geostationary Lightning Mapper (GLM: Goodman et al., 2013; Rudlosky et

al., 2019) in certain types of storms with problematic precipitation structures (Bitzer, 2019; Said and Murphy, 2019; Thomas, 2019; Rutledge et al., 2019).

The attenuation of the optical lightning signals by the cloud medium suggests that optical space-based lightning detectors have more to gain from optimizing for sensitivity compared to other types of instruments – for examples, RF detectors. Scattering is particularly problematic for pixelated optical detectors compared to sensitive photodiode detectors, as the dispersed signal may be divided between pixels. This likely contributes to discrepancies between instruments noted in van der Velde and Montoyà (2020). Any improvements in sensitivity from lowering the detection threshold will allow the instrument to recover flashes that are obscured below optically thick clouds, while also resolving more of the lightning tree in all flashes. The primary concern in lowering the threshold is a dramatic increase in solar artifacts (Peterson, 2020c) and noise events. However, the potential benefits of such an optimized threshold for GLM's diverse collection of operational products have not been fully quantified.

The GLM threshold affects not only how much of the flash can be detected from space, it also limits the amount of thundercloud illumination that is measured from orbit. Scattering interactions allow optical lightning sources to illuminate the cloud scene far beyond the extent of the lightning tree. The most powerful groups detected by the Lightning Imaging Sensor (LIS: Christian et al., 2000; Blakeslee et al., 2020) and GLM encompass 10,000+ km^2 of the cloud-top (Peterson et al., 2017) – and include large areas of lower clouds that can transmit low-altitude lightning emissions or reflect high-altitude lightning emissions to provide a "shortcut" path to the satellite compared to traversing the full optical depth of convective cloud (Peterson, 2019a; Peterson et al., 2020b). Much of this neighboring cloud illumination is sufficiently dim to quickly fall below higher thresholds.

This is the second part of our thundercloud illumination study. In Part 1 (Peterson et al., 2021a), we examined how the positions and geometries of optical sources affected GLM measurements of cloud illumination. In Part 2, we shift our focus from the emitter to the GLM instrument and quantify the effects of the GLM threshold on event / group detection, flash clustering, and gridded product generation. We take the Colombia thunderstorm from Part 1 that had a low GLM threshold of ~0.7 fJ, impose artificial thresholds on the event data between 1 fJ and 10 fJ, and then recompute the GLM cluster feature and gridded products using only the events above the imposed threshold. Changes in lightning rates and flash characteristics are discussed, along with how these changes affect the products downstream.

2 Data and Methodology

This study will use the matched GLM and LMA data from Part 1 that describes lightning activity in two thunderstorms (one in Colombia and the other in Colorado) to examine the effect of the GLM threshold on each type of GLM data product. The primary focus will be on the Colombia thunderstorm that was close to the GOES-16 satellite subpoint and had a low overall instrument threshold. With this low threshold, we can impose artificial event energy thresholds on the GLM data to determine how higher thresholds would impact detection, clustering, and gridded product generation for the same thunderstorm. Data from the Colorado thunderstorm will also be shown, but only as a point of reference for an observed case with a high threshold.

2.1 The GOES-16 Geostationary Lightning Mapper

GLM is a staring imager that records cloud-top illumination in a narrow spectral band around the 777.4 nm Oxygen emission line triplet at 500 frames per second (Goodman et al.,

2013). Transient changes in cloud-top illumination characteristic of lightning are detected by subtracting the estimated background brightness of a given pixel from the pixel energy recorded during a 2-ms integration frame, and then comparing the remaining signal energy with the current local instrument threshold. If the recorded energy is greater than the threshold, the instrument will trigger and report an event at that pixel. These pixel events are then clustered into higher-level features that describe lightning - including "groups" (which approximate lightning pulses) and flashes (Goodman et al., 2010; Mach, 2020). This cluster data is then used to construct GLM gridded products such as Flash Extent Density (FED), Average Flash Area (AFA), and Total Optical Energy (TOE) (Bruning et al., 2019).

The GLM data produced and distributed by NOAA, however, is subject to the limitations in the Lightning Cluster Filter Algorithm (LCFA: Goodman et al., 2010), which must run in an operational setting with strict latency requirements. To ensure timely data, the LCFA imposes arbitrary limits on group and flash clusters that prevent them from becoming too large or complex. These thresholds (101 events per group, 101 groups per flash, and a maximum flash duration of 3 s) are rather low compared to even LIS flashes (Peterson et al., 2017), and cause the most exceptional cases of lightning (i.e., Peterson et al., 2020a) to be artificially split into multiple pieces that are flagged as a "degraded" quality in the operational GLM data. To recover these flashes, Peterson (2019) developed methods that can be applied in post-processing to repair the flash cluster data and generate science-quality GLM data. This data is available at Peterson (2021a). As in Part 1, we use the repaired data here rather than the operational LCFA data.

2.2 Approximating GLM Thresholds and Imposing Artificial Thresholds

While the threshold at each pixel is not specified for GLM events, threshold values can be estimated from the lowest-energy events reported by GLM (Figure 1a in Peterson and Lay, 2019). If GLM can detect events from a thunderstorm down to 1 fJ, then the threshold must be somewhere below (and probably close to) 1 fJ – otherwise dimmer events would be reported. These estimates allow us to examine relative differences in threshold from storm to storm and from region to region, and to trend thresholds over time. However, minimum event energy is not a perfect approximation to the threshold at the pixel level. Radiative transfer across the cloud scene affects the energy distribution of recorded events. For example, cloud regions that do not produce lightning still can be illuminated by very bright lightning pulses from a nearby thunderstorm (i.e., Peterson et al., 2017). If these are the only optical pulses that generate GLM events in a particular pixel, then the minimum reported energy will be quite high compared to pixels in the nearby thunderstorm core. In the storm core, meanwhile, at least some of the lightning pulses will be rather dim, producing events near the actual threshold.

In the absence of an optical phenomenon that is known to significantly raise the local GLM threshold (an example being sustained illumination from solar glint: Peterson, 2020c), the actual threshold should not be substantially different between neighboring cloud regions that are subject to the same background illumination. Thus, the minimum event energies over a flash- or convective-scale region are expected to be a better approximation for the nominal threshold throughout that region than the minimum energies reported at each pixel. We use the flash minimum event energy per flash as our threshold proxy in this study.

Artificial thresholds above the local instrument threshold are applied to the GLM detections by collecting all the event data from the Colombia thunderstorm, removing detections that are less energetic than the chosen artificial threshold, and then reconstructing the derived

GLM data products from the events that exceed the new threshold (for example, the meteorological imagery in Bruning et al., 2019). We consider artificial thresholds between 1 fJ and 10 fJ in this study, which correspond to typical GLM thresholds over the regions across the Americas where lightning is most common (i.e., Figure 1 in Rudlosky et al., 2019; Figure 5 in Peterson, 2019). Higher minimum event energy values are found at the edge of the instrument FOV, but these likely result from biases in the pixel energy distributions from the near side-view of thunderstorms in these regions rather than the true local instrument threshold. Thus, higher thresholds will not be considered.

The removal of dim events and groups under higher thresholds can cause single flashes to become split if the remaining groups / events no longer meet the LCFA clustering criteria. While higher thresholds reduce the number of flashes detected by GLM, flash splitting artificially increases the number of flashes that would be detected. As these split flashes do not represent physically distinct features, we examine the effect of this splitting separately from the loss of GLM detections. Section 3.2 examines the consequences of event / group / flash losses under each threshold using the original cluster data that best captures the physical development of each flash. Then, Section 3.3 examines how flash splitting modifies these results by constructing new cluster data using the remaining events at each artificial threshold.

3 Results

3.1 GLM Thresholds in Colorado and Colombia Thunderstorms

GLM is known to have a relatively high threshold in parts of Colorado. To test this assertion and quantify differences in threshold between the Colorado and Colombia

thunderstorms, we construct timeseries of minimum GLM event energies in Figure 1 for the Colombia (Figure 1a) and Colorado (Figure 1b) thunderstorms. As in the timeseries in Figure 1 (Colombia) and Figure 3 (Colorado) in Part 1, times are relative to 00:00 UTC on the first day of the storm (11/1/2019 for Colorado and 7/1/2019 in Colorado), and only GLM lightning activity in the LMA data domain (defined by latitude and longitude boxes) are shown. The red timeseries in Figure 1 show the minimum GLM event energy for any pixel within the LMA data domain, while the dark blue timeseries averages the minimum event energies across all pixels with lightning in the domain, and the light blue timeseries shows the maximum value of minimum event energy in any pixel. Horizontal lines are drawn to show constant energies from 1-5 fJ (solid) as well as 10 and 100 fJ (dashed).

We noted in Part 1 that there were periods of time during the Colorado storm where lightning activity occurred in the warmer clouds surrounding deep convection, but not in the thicker convective clouds, themselves. This indicates that the sample of lightning measured by GLM will be biased towards the brighter flashes and the minimum pixel energy in these peripheral regions is not expected to be the best representation of the actual GLM threshold. Throughout the timeseries in Figure 1b, the lowest event energies (red) range from <1 fJ to nearly 5 fJ, while the maximum pixel values of minimum event energy reach 70 fJ - causing average pixel values to range from 5 to 10 fJ. The minimum event energy also varies according to time of day, with the red curve starting at 5 fJ in the late afternoon and largely decreasing below 2 fJ after nightfall. Examining changes in flash count and Total Optical Energy (TOE) after imposing artificial thresholds between 1 fJ and 10 fJ (not shown for the Colorado case) indicates that the overall effective threshold for the Colorado thunderstorm was between 3 and 4 fJ, as this is the point where notable changes in the GLM detection totals begin to occur.

Thresholds in the 3-4 fJ range are still relatively high for GLM. The Colombia case (Figure 1a) is expected to have a low threshold due to its proximity to the satellite subpoint. Indeed, the lowest event energies (red curve) during the most active storm period (6-11 UTC) are universally below 1 fJ. As before, certain pixels have greater minimum event energy values (light blue curve) up to 30 fJ, and these impact the overall domain mean (blue curve). However, the overall effective GLM threshold for the region is inferred to be < 1 fJ, and probably close to the ~0.7 fJ average for the red curve during this period.

3.2 The effect of GLM Threshold on Event / Group / Flash Detection

Artificial thresholds of between 1 fJ and 10 fJ are imposed on the GLM event data from the Colombia thunderstorm to determine how many of the original flashes are removed by increasing the threshold. Figure 2 shows how event count (a), group count (b), flash count (c), and TOE (d) change under each imposed threshold. Solid lines include all the GLM data, while the dashed lines do not consider data from single-group flashes that are removed by the current version of the LCFA (Rudlosky and Virts, 2021). As minimum event energy values were close to 1 fJ in Figure 2e, there is little difference between no imposed threshold (0 fJ) and a 1 fJ threshold in any of the plots. However, increasing the threshold just to 2 fJ severely impacts event detection (Figure 2a). By a 4 fJ threshold (comparable to the Colorado case), 70% of the original events have been eliminated, while 90% of events are missed under a 10 fJ threshold.

The loss of these dim events under higher thresholds affects group and flash detection, TOE, and the characteristics of the remaining groups and flashes. Overall group counts (Figure 2b) are reduced by 25% under a 2 fJ threshold, 55% by 4 fJ, and 81% by 10 fJ. TOE (Figure 2d), meanwhile, is reduced by 12% by 2 fJ, 29% by 4 fJ, and 53% by 10 fJ. The TOE values in

Figure 2d accumulate all events from the Colombia thunderstorm, but TOE is also reported as a gridded product. The severe losses in TOE at the storm level between a 1 fJ and 10 fJ threshold are the first indication that changing thresholds will become important when trending GLM grids.

Of the four parameters considered in Figure 2, flash count (Figure 2c) is the key metric for GLM performance, and it is least impacted by thresholds changes. Only 4% of the original flashes (solid line) are lost by increasing the threshold to 2 fJ, 15% by 4 fJ, and 35% by 10 fJ. Many of these flashes are reduced to a single group, however, and would not be reported by the LCFA. Removing these flashes (dashed line) increases the overall losses to 7% by 2 fJ, 20% by 4 fJ, and 44% by 10 fJ. Still, these losses are small compared to the total event and group counts and thunderstorm TOE values in Figure 2, suggesting that the primary effect of an increased threshold is the loss of the flash detail and the extent of cloud illumination that can be resolved.

Figure 3 shows the remaining groups that do not fall completely below threshold and plots histograms of group energy (Figure 3a) and group footprint area (Figure 3b) (as a percent of the original group area / energy) under thresholds ranging from 1 fJ to 10 fJ. For each threshold, the horizontal bins in Figure 3 sum to 100%. Percentiles are also tracked between thresholds with line overlays. While these groups are still resolved by GLM, their appearance is significantly modified under the increased thresholds. The median group energy declines to two-thirds of the energy of the original group, while the median group area is reduced to one-fourth of the original group area. However, not all groups are affected in the same way, leading to a broad range of possible energy reductions under higher thresholds. While some groups lose virtually none of their original energy by 10 fJ, others lose 95%.

The group area distributions in Figure 3b show that the loss of faint events at higher

thresholds causes the group area to be substantially eroded. While quantization from an integer number of illuminated pixels limits the possible values and causes percentages that correspond to rational numbers (i.e., 25%, 50%) to stand out, the distributions still show that group area is more sensitive to threshold effects than group energy. This is because most of the events that comprise a group are rather dim compared to the brightest event in the group. A point source within a cloud may consist of a single bright event in the pixel over the source with a surrounding ring of dim events. In this case, there will be one brighter event, and then eight dim events in the ring. Thus, the dim pixels in a group will far outnumber the bright pixels. Even increasing the threshold slightly to 2 or 3 fJ severely impacts the detection of peripheral dim events, and the median group area is reduced by half while the median group energy only declines by 12%. Under the highest thresholds, groups might only contain the single brightest event.

To determine what this event loss does to flash characteristics, Figure 4 repeats the analysis from Figure 3 at the flash level. Flashes must have at least one event above the maximum threshold (10 fJ) to be considered, and all groups that fall below the threshold will not contribute to the flash energy (Figure 4a) or flash area (Figure 4b). The key difference between the group level (Figure 3) and the flash level (Figure 4) characteristics is the notable lack of flashes that are virtually unchanged from the original threshold. Even moderate thresholds of 2-3 fJ are sufficient to erode much of the flash energy and at least some of the flash area.

The reductions in flash energy are more severe than group energy losses because flashes are comprised mostly of small dim groups offset by a few bright pulses (Peterson et al., 2018). While individually dim, the total energy from these pulses has a significant impact on the overall flash energy - and they are removed entirely under these higher thresholds alongside the dim

289 portions of the brighter groups. The flash area reductions, meanwhile, are comparable to the
290 group area reductions that we saw previously in Figure 3. This is probably not a coincidence, as
291 flash area is often determined by the largest group in the flash (Peterson et al., 2017). Lateral
292 propagation only plays a central role in determining flash area once the group separation exceeds
293 the scale of these brighter individual GLM groups.
294
295 *3.3 The effect of GLM Threshold on Flash Clustering*
296 The complete loss of dim groups and erosion of brighter groups under an increased
297 threshold poses a challenge for GLM lightning mapping and flash clustering. Flash structure is
298 mapped by tracking the faint localized discharges that occur along the developing branches of
299 the flash. As these events fall below threshold, the GLM maps resolve flash structure using an
300 increasingly-smaller number of points – adding uncertainty to the path that was taken by the
301 flash through the cloud. Eventually, the removal of these dim events will reach a point where the
302 remaining events become separated in space and time beyond the thresholds used by the GLM
303 clustering algorithm (Goodman et al., 2010). This causes the original single lightning flash to be
304 split into multiple flash features that represent different illuminated portions of the lightning tree.
305 Figure 5 demonstrates how increasing the threshold affects clustering using the case of a
306 long horizontal lightning flash from the Colombia thunderstorm. The flash is mapped with a
307 color contour representing the TOE from only the flash in question, and with a line segment
308 overlay connecting subsequent groups in the flash. If the original flash becomes split into
309 multiple flash features, each of these split flashes will be assigned a different color for the group
310 line segment overlay. Index numbers for each split flash are also drawn in its assigned color. The
311 flash is plotted under the original threshold in Figure 5a. Most of the group activity in the flash

312 occurred along its southern flank, while a linear branch can also be noted extending to the
313 northeast. TOE values were reasonably-high over most of the flash footprint (i.e., > 100 fJ) - but
314 note that these are summed over all events, which can mask large numbers of events that are
315 removed under the higher thresholds.

316 Figure 5b removes all events below a 3 fJ threshold and then reclusters the flash using the
317 remaining events. While the flash extent is reduced under this higher threshold due to the loss of
318 groups at the ends of the southern and northeastern branches, the overall flash structure is mostly
319 intact. However, the large distance between some of the groups (i.e., long straight lines in Figure
320 5b) - particularly along the northern branch - signify that the group separations are approaching
321 the limits of the clustering algorithm (16.5 km, 330 ms). The clustering algorithm still clusters
322 these groups into a single flash at this point because GLM clustering depends on the separation
323 of events within a group and not the separations of group centroids that are depicted by the line
324 segments. Still, the large group spacing indicates that we have limited information about how the
325 northern branch of the flash developed, and further increasing the threshold is likely to result in
326 splitting.

327 Figure 5c increases the threshold up to 6 fJ, causing in the first split section from the
328 original flash. Removing the events below this threshold prevents most of the development of the
329 northern branch from being resolved. The branch is still evident as a contiguous feature in the
330 TOE plot, but the individual groups that would be detected by GLM are too far apart in space
331 and time to meet the GLM definition of a flash. Thus, the collection of groups at the far end of
332 the branch are split into a distinct flash feature (depicted with blue line segments and assigned an
333 index of 2) from the primary flash (colored black with the original index of 1). Continuing to
334 increase the threshold to 9 fJ (Figure 6d) splits the northern branch of the flash further into a

third central piece (colored red with an index of 3). Thus, we have the primary flash (black), the larger central split flash (red) and the original split flash at the end of the branch (blue) – which has been reduced to a single point and would not be reported by the current version of the LCFA, as it filters out these single-group flashes.

Flash splitting artificially increases thunderstorm flash counts. Long horizontal flashes like the case in Figure 5 are particularly problematic because their lateral development makes them prone to being broken into multiple small pieces (as we saw in Figure 5d) rather than two roughly equal sized pieces. Moreover, as these flashes occur outside of the convective core where flash rates are generally low to begin with, any splitting will noticibly alter the local flash rate. The scale of this problem is demonstrated in Figure 6 by quantifying flash splitting frequency at each flash size and imposed threshold. Flash splitting is not a severe issue for convective-scale flashes (i.e., ~10 km in size), as < 10% of flashes are split at any threshold. However, when flashes grow to 50-km, more than half are split at the higher thresholds (i.e., >3 fJ) and nearly 80% of the largest flashes (100+ km) at the highest thresholds (5-10 fJ) are split.

It is not immediately clear how much the threshold-based splitting will change the overall flash rate for a given thunderstorm because the larger flashes that are frequently split are far less common than the convective-scale flashes that remain intact at higher thresholds. To assess the impact of splitting on the flash rates from the Colombia thunderstorm, Figure 7a counts the number of reclustered flashes at each threshold and compares this number to the original flash counts from Figure 2c. As before, we consider both the case of all flashes (solid lines) and multi-group flashes (dashed lines) that are not removed by the current LCFA. When the imposed threshold is near the instrument threshold (i.e., 0 fJ – 1 fJ), the original (black curves) and reclustered (blue curves) flash counts are nearly identical. However, imposing a 2 fJ or higher

358 threshold causes the reclustered curves to increase beyond the original flash count curves. All the
359 curves in Figure 7a decrease at higher thresholds as whole flashes fall below the threshold, but
360 the separation in the curves remains fairly constant. Figure 7b quantifies this by computing the
361 ratios between the reclustered flash counts and the original flash counts at each threshold. Flash
362 splitting artificially increases the overall flash rate from the Colombia thunderstorm by 6% for all
363 flashes and 3% for multi-group flashes under a 2 fJ threshold, 9% and 6% under a 4 fJ threshold,
364 and 12% and 7% under a 10 fJ threshold. These increases partially counteract the 35% (all
365 flashes) and 44% (multi-group flashes) loss in flash count over the same threshold range that we
366 described in Figure 2c, but these apparent improvements in the detected flash rates are only the
367 result of artificial biases in the GLM data.
368
369 *3.4 The effect of GLM Threshold on Gridded Product Generation*
370 The GLM threshold affects the gridded products generated from flash cluster data by
371 combing the effects discussed in the previous sections. These include:
372 (1) Removing below-threshold events at the periphery of the flash / group footprints
373 reduces the spatial extent of features in the gridded data.
374 (2) Eliminating below-threshold events modifies the flash characteristics represented in
375 the grids – both in the original sample of flashes, and following the threshold-based
376 artificial flash splitting.
377 (3) Removing below-threshold events / groups / flashes modifies the sample of lightning
378 used to generate the grids - introducing a bias towards the more prominent flashes
379 that can survive the removal of below-threshold events (including the LCFA removal
380 of single-group flashes).

While the degree to which the above effects impact the GLM gridded products differs from grid to grid, it generally depends on whether the grid is generated by summing / averaging flash characteristics (i.e., TOE, FED, AFA, Average Flash Extent, Average Flash Duration) or by looking at their minimum values (i.e., Minimum Flash Area: MFA). Grids based on maximum flash characteristics are not considered here but would more closely resemble the total / mean grids than the minimum grids. We elect to discuss two representative grids that demonstrate these effects – AFA and MFA – and provide the remaining grids as Supporting Information. All of these grids are generated using only multi-group flashes that would not be removed by the LCFA.

AFA grids are shown in Figure 8 for imposed thresholds between 0 fJ and 10 fJ, with an increment of 2 fJ between panels. Note that an exponential scale is used to capture the large dynamic range of GLM flash areas, so even slight changes in color represent a notable difference in flash size. When no artificial threshold is imposed, flash sizes within the primary storm feature at the center of the image range from 600 km^2 at its center to over 5,000 km^2 at its northwest edge. This behavior is largely due flashes of all energies illuminating the convective core of the thunderstorm while the brightest flashes can also illuminate neighboring clouds - but long horizontal flashes can also contribute to larger flash areas in these non-convective regions.

Imposing a threshold of even 2 fJ (Figure 8b) removes much of the illumination around the edge of the thunderstorm feature, while causing all AFA values to decrease. The largest AFA values are around 3000 km^2 while the convective core sees its first pixels in the 300-600 km^2 range. Increasing the threshold further from 4 fJ up to 10 fJ (Figure 9c-f) continues these trends: the thunderstorm feature becomes smaller while the AFA values continue to decline. What was initially a region of small flashes surrounded by larger flash areas under a < 1 fJ threshold is

reduced to a cluster of small flashes by 10 fJ with only a few pixels of increased flash areas on the northwestern flank to indicate the larger flash areas from the original grid.

These changes in AFA are modest compared to grids that examine minimum values like MFA. Figure 9 shows the MFA grids at each threshold level during the same thunderstorm snapshot as Figure 8. Removing dim GLM events has greater effect on MFA because only the brightest events in the groups that comprise a given flash might exceed the imposed threshold. Thus, while the initial MFA grid in Figure 9a might resemble an amplified version of the AFA grid in Figure 8 that emphasizes the small flashes in the convective core and the larger flashes that illumine its periphery, minimum flash sizes quickly fall off across the thunderstorm feature as thresholds are increased beyond 2 fJ (Figure 9c-f). By a 10 fJ threshold, nearly half of the gridpoints within the feature correspond to flashes consisting of only 1-pixel GLM flashes, and the remainder are < 200 km^2 in size.

These variations in AFA and MFA with threshold demonstrate the challenge of trending GLM gridded products over time. Thresholds usually change from day to night and, as we saw in Figure 1b for the Colorado case, these changes can extend over multiple femtojoules of event energy. This is further complicated by threshold differences across the GLM imaging array (i.e., between RTEPs). As storms move and develop over time, the characteristics of their flashes will change, driving trends in the GLM gridded products. But these trends will be confounded by any changes in threshold that occur over the same period. To mitigate threshold biases in gridded product trends, it is necessary to construct grids that remain consistent over the life cycle of the storm in question. Imposing artificial thresholds at the highest threshold values encountered by the storm of interest, as we have done here, is one way of doing this. However, this comes with the cost of losing much of the flash detail that is required to measure the flash characteristics

being trended.

4 Conclusion

This second part of our thundercloud illumination study focuses on the effect that the GLM instrument threshold has on GLM data products. To quantify threshold effects, we consider a thunderstorm that occurred with a low instrument threshold (~0.7 fJ), impose artificial thresholds over the range of 1 fJ to 10 fJ, and then examine how each type of GLM data product is modified by these threshold changes.

The primary effect of the threshold-based changes to the GLM products is the loss of faint events that are present under lower thresholds. Losing the below-threshold dim events erodes the footprints of GLM groups and flashes until they fall completely below the higher threshold and go undetected. As flashes are comprised primarily of dim events and groups offset by a few energetic pulses, increasing the instrument threshold has a greater impact on event and group detection than on flash detection. Imposing a 2 fJ artificial threshold on our thunderstorm case decreases the event count by 60% compared to the original data, while imposing a 10 fJ threshold removes 90% of the original events. Meanwhile, 25% of groups are removed with a 2 fJ threshold and 81% are lost under a 10 fJ threshold.

The threshold effect on flash detection is complicated by losing dim events and groups that can result in flash splitting as the remaining events and groups exceed the space and time thresholds employed by the GLM clustering algorithm. Of the original GLM flashes, 4% fall completely below a 2 fJ threshold and 35% are eliminated by a 10 fJ threshold. The current version of the GLM LCFA also removes single-group flashes. Filtering out these flashes

449 increases the threshold-induced losses to 7% by 2 fJ, 20% by 4 fJ, and 44% by 10 fJ. At the same
450 time, flash splitting artificially increases the overall flash count by 6% at 2 fJ and up to 12% by
451 10 fJ and the multi-group flash count by 3% at 2 fJ and up to 9% by 10 fJ.

452 Gridded products generated from GLM flash cluster data are also severely impacted by a
453 combination of missed / split flashes and reductions in the flash / group footprints at higher
454 thresholds. We consider the AFA and MFA products as representative of total / mean /
455 maximum products (AFA) and minimum products (MFA) and examine how they change
456 under the imposed thresholds. The size of the GLM feature describing the illuminated
457 thunderstorm decreased under higher thresholds, as illumination around the periphery of the
458 storm core from distant bright / large flashes quickly falls below threshold. Flash sizes within the
459 storm core also generally decreased due to smaller flashes losing portions of their footprints, and
460 flash splitting. The key difference between AFA and MFA is the scale of this reduction in area.
461 As MFA examines the minimum flash area, flashes comprised of a few events just above the
462 threshold can report flash areas corresponding to just 1 or 2 GLM pixels. This is problematic for
463 non-convective storm regions that produce large lightning flashes, as these long horizontal
464 flashes are more prone to splitting at higher thresholds than small convective-scale flashes.

465 These results demonstrate the importance of considering the context surrounding GLM
466 detections – the configuration of the cloud scene, corresponding instrument threshold, location,
467 and time of day, etc. - when interpreting GLM data. This is particularly important when
468 accumulating data from a diverse collection of lightning flashes (for example, when generating
469 gridded products) or trending GLM data over time. Changes in the situational context (for
470 example, spatial / diurnal changes in threshold) can have a considerable impact on the results.

Future work in Part 3 (Peterson et al., 2021b), will leverage these results to show how the altitude of the source within the cloud can be estimated from group-level cloud illumination metrics. Finally, Part 4 (Peterson et al., 2021d) will evaluate volumetric meteorological and thundercloud imagery derived from GLM data.

Acknowledgments

This work was supported by the US Department of Energy through the Los Alamos National Laboratory (LANL) Laboratory Directed Research and Development (LDRD) program under project number 20200529ECR. Los Alamos National Laboratory is operated by Triad National Security, LLC, for the National Nuclear Security Administration of U.S. Department of Energy (Contract No. 89233218CNA000001). The work by co-author Douglas Mach was supported by ASA 80MFSC17M0022 "Cooperative Agreement with Universities Space Research Association" and NASA Research Opportunities in Space and Earth Science grant NNX17AJ10G "U.S. and European Geostationary Lightning Sensor Cross-Validation Study." We would like to thank the operators of the Colorado LMA at Colorado State University and the Colombia LMA at the Technical University of Catalonia, and Drs. Ken Cummins and Jesús López for sharing their processed LMA data for the presented cases. The data used in this study is available at Peterson (2021b).

References

Bitzer, P. M., (2019). The fruit basket of GLM detection efficiency. *GLM Science Team Meeting, 2019.* Huntsville, AL, USA, 33 slides. Available online at: https://goes-r.nsstc.nasa.gov/home/sites/default/files/2019-09/Bitzer_20190912_glm_sci_mtg.pptx.

Blakeslee, R.J., Lang, T.J., Koshak, W.J., Buechler, D., Gatlin, P., Mach, D.M., Stano, G.T., Virts, K.S., Walker, T.D., Cecil, D.J., Ellett, W., Goodman, S.J., Harrison, S., Hawkins, D.L., Heumesser, M., Lin, H., Maskey, M., Schultz, C.J., Stewart, M., Bateman, M., Chanrion, O. and Christian, H. (2020), Three Years of the Lightning Imaging Sensor Onboard the International Space Station: Expanded Global Coverage and Enhanced Applications. *J. Geophys. Res. Atmos*., **125**: e2020JD032918. https://doi.org/10.1029/2020JD032918

Brunner K., & P. M. Bitzer (2020). A first look at cloud inhomogeneity and its effect on lightning optical emission. *Geophysical Research Letters*, 47, e2020GL087094. https://doi.org/10.1029/2020GL087094

Bruning, E., Tillier, C. E., Edgington, S. F., Rudlosky, S. D., Zajic, J., Gravelle, C., et al. (2019). Meteorological imagery for the geostationary lightning mapper. *Journal of Geophysical Research: Atmospheres*, 2019; 124: 14285– 14309. https://doi.org/10.1029/2019JD030874

Christian, H. J., R. J. Blakeslee, S. J. Goodman, and D. M. Mach (Eds.), (2000). Algorithm Theoretical Basis Document (ATBD) for the Lightning Imaging Sensor (LIS), NASA/Marshall Space Flight Center, Alabama. (Available as http://eospso.gsfc.nasa.gov/atbd/listables.html, posted 1 Feb. 2000).

Goodman, S. J., R. J. Blakeslee, W. J. Koshak, D. Mach, J. Bailey, D. Buechler, L. Carey, C. Schultz, M. Bateman, E. McCaul Jr., and G. Stano, (2013). The GOES-R geostationary lightning mapper (GLM). *J. Atmos. Res.,* **125-126**, 34-49

Hutchins, M. L., Holzworth, R. H., Brundell, J. B., and Rodger, C. J. (2012), Relative detection efficiency of the World Wide Lightning Location Network, *Radio Sci.*, 47, RS6005, doi:10.1029/2012RS005049.

Jacobson, A.R., R. Holzworth, J. Harlin, R. Dowden, and E. Lay, 2006: Performance Assessment of the World Wide Lightning Location Network (WWLLN), Using the Los Alamos Sferic Array (LASA) as Ground Truth. *J. Atmos. Oceanic Technol.,* **23**, 1082–1092, https://doi.org/10.1175/JTECH1902.1

Jacobson, A. R., & Light, T. E. L. (2012). Revisiting" Narrow Bipolar Event" intracloud lightning using the FORTE satellite. In *Annales Geophysicae* (Vol. 30, No. 2, p. 389). Copernicus GmbH.

Koshak, W. J., Solakiewicz, R. J., Phanord, D. D., and Blakeslee, R. J. (1994), Diffusion model for lightning radiative transfer, *J. Geophys. Res.*, 99(D7), 14361– 14371, doi:10.1029/94JD00022.

Koshak, W. J. (2010). Optical Characteristics of OTD Flashes and the Implications for Flash-Type Discrimination, *Journal of Atmospheric and Oceanic Technology*, *27*(11), 1822-1838. Retrieved Jan 21, 2021, from https://journals.ametsoc.org/view/journals/atot/27/11/2010jtecha1405_1.xml

Lang, T. J., Pédeboy, S., Rison, W., Cerveny, R. S., Montanyà, J., Chauzy, S., ... & Krahenbuhl, D. S. (2017). WMO world record lightning extremes: Longest reported flash distance and longest reported flash duration. *Bulletin of the American Meteorological Society*, *98*(6), 1153-1168.

Lay, E. H., Holzworth, R. H., Rodger, C. J., Thomas, J. N., Pinto, O., and Dowden, R. L. (2004), WWLL global lightning detection system: Regional validation study in Brazil, *Geophys. Res. Lett.*, 31, L03102, doi:10.1029/2003GL018882.

Light, T. E., Suszcynsky, D. M., and Jacobson, A. R. (2001a), Coincident radio frequency and

optical emissions from lightning, observed with the FORTE satellite, *J. Geophys. Res.*, 106(D22), 28223– 28231, doi:10.1029/2001JD000727.

Light, T. E., Suszcynsky, D. M., Kirkland, M. W., and Jacobson, A. R. (2001b), Simulations of lightning optical waveforms as seen through clouds by satellites, *J. Geophys. Res.*, 106(D15), 17103– 17114, doi:10.1029/2001JD900051.

Mach, D. M. (2020). Geostationary Lightning Mapper clustering algorithm stability. *Journal of Geophysical Research: Atmospheres*, 125, e2019JD031900. https://doi.org/10.1029/2019JD031900.

Peterson, M. (2019a). Using lightning flashes to image thunderclouds. *Journal of Geophysical Research: Atmospheres*, 124, 10175– 10185. https://doi.org/10.1029/2019JD031055

Peterson, M. (2019b). Research applications for the Geostationary Lightning Mapper operational lightning flash data product. *Journal of Geophysical Research: Atmospheres*, 124, 10205– 10231. https://doi.org/10.1029/2019JD031054

Peterson, M. (2020a). Modeling the transmission of optical lightning signals through complex 3-D cloud scenes. *Journal of Geophysical Research: Atmospheres*, 125, e2020JD033231. https://doi.org/10.1029/2020JD033231

Peterson, M. (2020b). Holes in Optical Lightning Flashes: Identifying Poorly-Transmissive Clouds in Lightning Imager Data. *Earth and Space Science*, 7, e2020EA001294https://doi.org/10.1029/2020EA001294

Peterson, M. (2020c). Removing solar artifacts from Geostationary Lightning Mapper data to document lightning extremes. *Journal of Applied Remote Sensing*, *14*(3), 032402.

Peterson, M. (2021a). GLM-CIERRA http://dx.doi.org/10.5067/GLM/CIERRA/DATA101

Peterson, M. (2021b). Coincident Optical and RF Lightning Detections from a Colombia Thunderstorm. https://doi.org/10.7910/DVN/5FR6JB, Harvard Dataverse, V1

Peterson, M., & Lay, E. (2020). GLM observations of the brightest lightning in the Americas. *Journal of Geophysical Research: Atmospheres*, 125, e2020JD033378. Peterson, M. J., Lang, T. J., Bruning, E. C., Albrecht, R., Blakeslee, R. J., Lyons, W. A., et al. (2020a). New World Meteorological Organization certified megaflash lightning extremes for flash distance (709 km) and duration (16.73 s) recorded from space. *Geophysical Research Letters*, 47, e2020GL088888. https://doi.org/10.1029/2020GL088888

Peterson, M., Rudlosky, S., & Deierling, W. (2017). The evolution and structure of extreme optical lightning flashes. *Journal of Geophysical Research: Atmospheres*, 122, 13,370–13,386. https://doi.org/10.1002/2017JD026855

Peterson, M., Rudlosky, S., & Deierling, W. (2018). Mapping the lateral development of lightning flashes from orbit. *Journal of Geophysical Research: Atmospheres*, 123, 9674–9687. https://doi.org/10.1029/2018JD028583

Peterson, M., Rudlosky, S., & Zhang, D. (2020b). Changes to the appearance of optical lightning flashes observed from space according to thunderstorm organization and structure. *Journal of Geophysical Research: Atmospheres*, 125, e2019JD031087. https://doi.org/10.1029/2019JD031087

Peterson, M., Light, T., & Mach, D. (2021a). The Illumination of Thunderclouds by Lightning: Part 1: The Extent and Altitude of Optical Lightning Sources. *Journal of Geophysical Research: Atmospheres*.

Peterson, M., Light, T., & Mach, D. (2021b). The Illumination of Thunderclouds by Lightning: Part 3: Retrieving Optical Source Altitude. *Journal of Geophysical Research: Atmospheres*.

Peterson, M., & Mach, D. (2021c). The Illumination of Thunderclouds by Lightning: Part 4: Volumetric Thunderstorm Imagery. *Journal of Geophysical Research: Atmospheres*.

Rison, W., Thomas, R. J., Krehbiel, P. R., Hamlin, T., & Harlin, J. (1999). A GPS-based three-dimensional lightning mapping system: Initial observations in central New Mexico. *Geophysical research letters*, *26*(23), 3573-3576.

Rudlosky, S. D., S. J. Goodman, K. S. Virts, and E. C. Bruning, (2019). Initial geostationary lightning mapper observations. *Geophys. Res. Lett.*, **46**, 1097– 1104. https://doi.org/10.1029/2018GL081052

Rudlosky, S. D. and K. S. Virts, (2021). Dual Geostationary Lightning Mapper Observations. Mo. Wea. Rev., 149, 979-998, https://doi.org/10.1175/MWR-D-20-0242.1.

Rutledge, S. A., K. Hilburn, A. Clayton, & B. Fuchs, (2019). CSU GLM work summary. *GLM Science Team Meeting, 2019.* Huntsville, AL, USA, 20 slides. Available online at: https://goes-r.nsstc.nasa.gov/home/sites/default/files/2019-09/GLM%20presentation%20Sept%202019_FINAL.pptx.

Rodger, C. J., Werner, S., Brundell, J. B., Lay, E. H., Thomson, N. R., Holzworth, R. H., & Dowden, R. L. (2006, December). Detection efficiency of the VLF World-Wide Lightning Location Network (WWLLN): initial case study. In *Annales Geophysicae* (Vol. 24, No. 12, pp. 3197-3214). Copernicus GmbH.

Said, R., & M. Murphey, (2019). Spatiotemporal patterns of GLM flash DE. *GLM Science Team Meeting, 2019.* Huntsville, AL, USA, 18 slides. Available online at: https://goes-r.nsstc.nasa.gov/home/sites/default/files/2019-09/Said_GLM_2019.pptx.

Thomas, R., (2019). Low GLM detection efficiencies in large storms. *GLM Science Team Meeting, 2019.* Huntsville, AL, USA, 18 slides. Available online at: https://goes-r.nsstc.nasa.gov/home/sites/default/files/2019-09/Thomas-GLM-sci-meeting-2019.pdf.

Thomson, L.W. and E.P. Krider, (1982). The Effects of Clouds on the Light Produced by Lightning. *J. Atmos. Sci.,* **39**, 2051–2065, https://doi.org/10.1175/1520-0469(1982)039<2051:TEOCOT>2.0.CO;2

van der Velde, O. A., Montanyà, J., Neubert, T., Chanrion, O., Østgaard, N., Goodman, S., et al. (2020). Comparison of high-speed optical observations of a lightning flash from space and the ground. *Earth and Space Science*, 7, e2020EA001249. https://doi.org/10.1029/2020EA001249

Zhu, Y., Rakov, V. A., Tran, M. D., Stock, M. G., Heckman, S., Liu, C., … Hare, B. M. (2017). Evaluation of ENTLN performance characteristics based on the ground truth natural and rocket-triggered lightning data acquired in Florida. *Journal of Geophysical Research: Atmospheres*, 122. 9858– 9866, https://doi.org/10.1002/2017JD027270

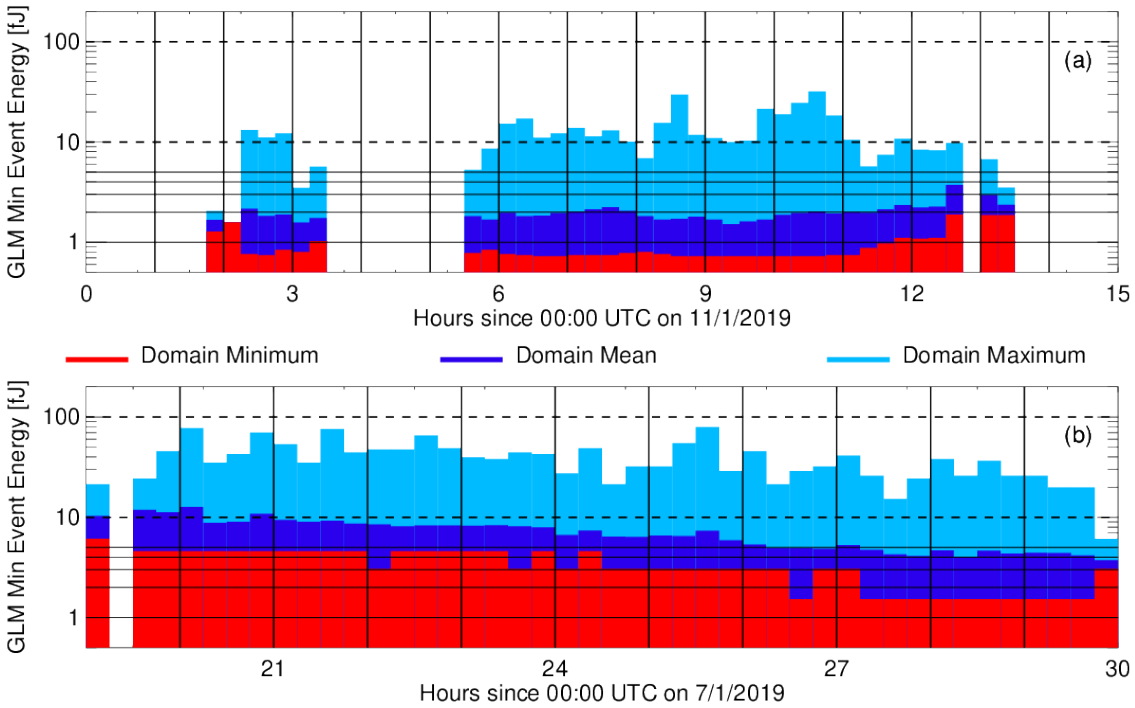

Figure 1. Timeseries of GLM minimum event energy during a thunderstorm over (a) Colombia near the satellite subpoint where thresholds are generally low and (b) Colorado where thresholds are known to be relatively high. Minimum event energies are computed for every pixel and the minimum (red), mean (dark blue) and maximum (light blue) values over each region are reported.

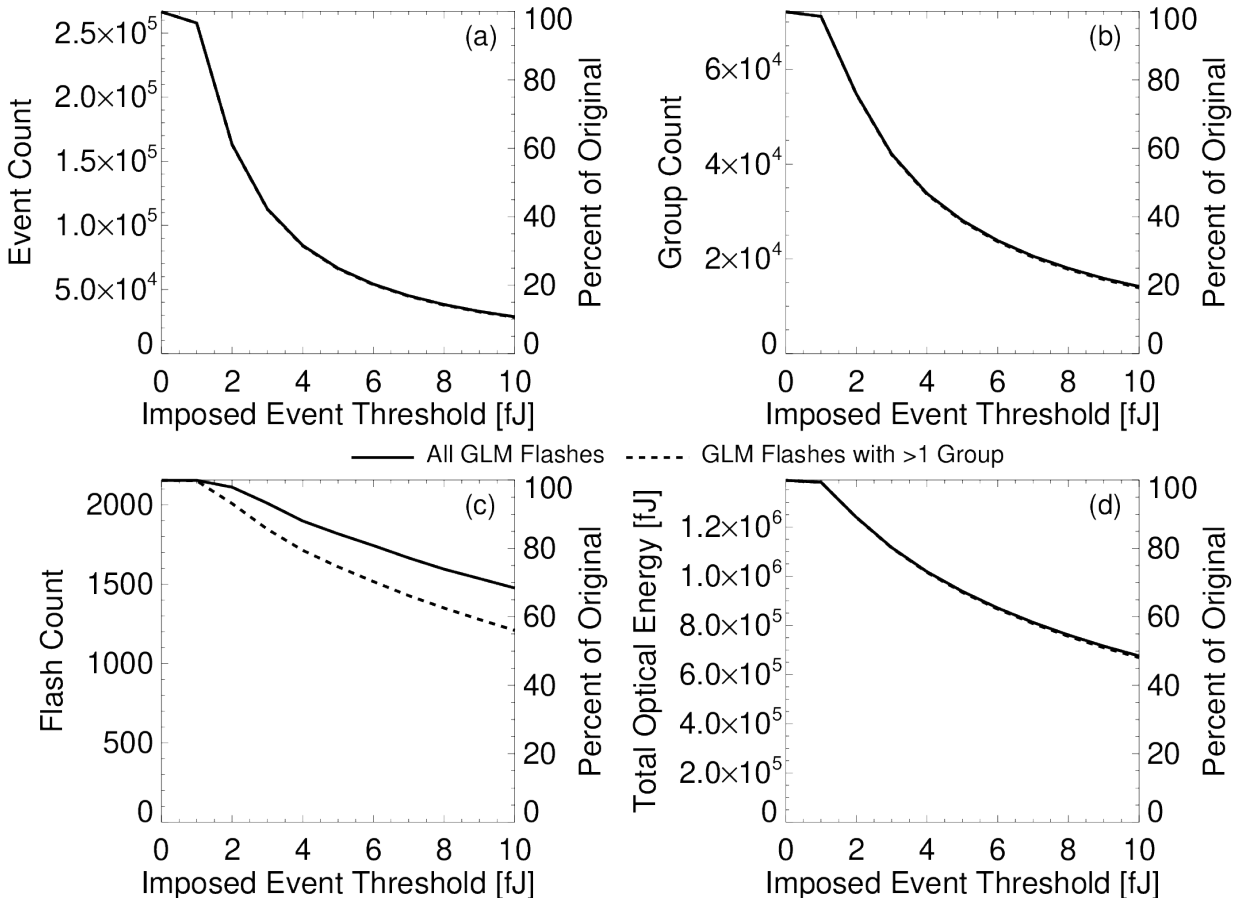

Figure 2. GLM (a) event, (b) group, and (c) flash counts, and (d) Total Optical Energies from the Colombia thunderstorm under artificial thresholds ranging from 0 fJ (original instrument thresholds) to 10 fJ. Solid curves indicate all GLM flashes while dashed curves only consider multi-group flashes that would not be removed by the LCFA.

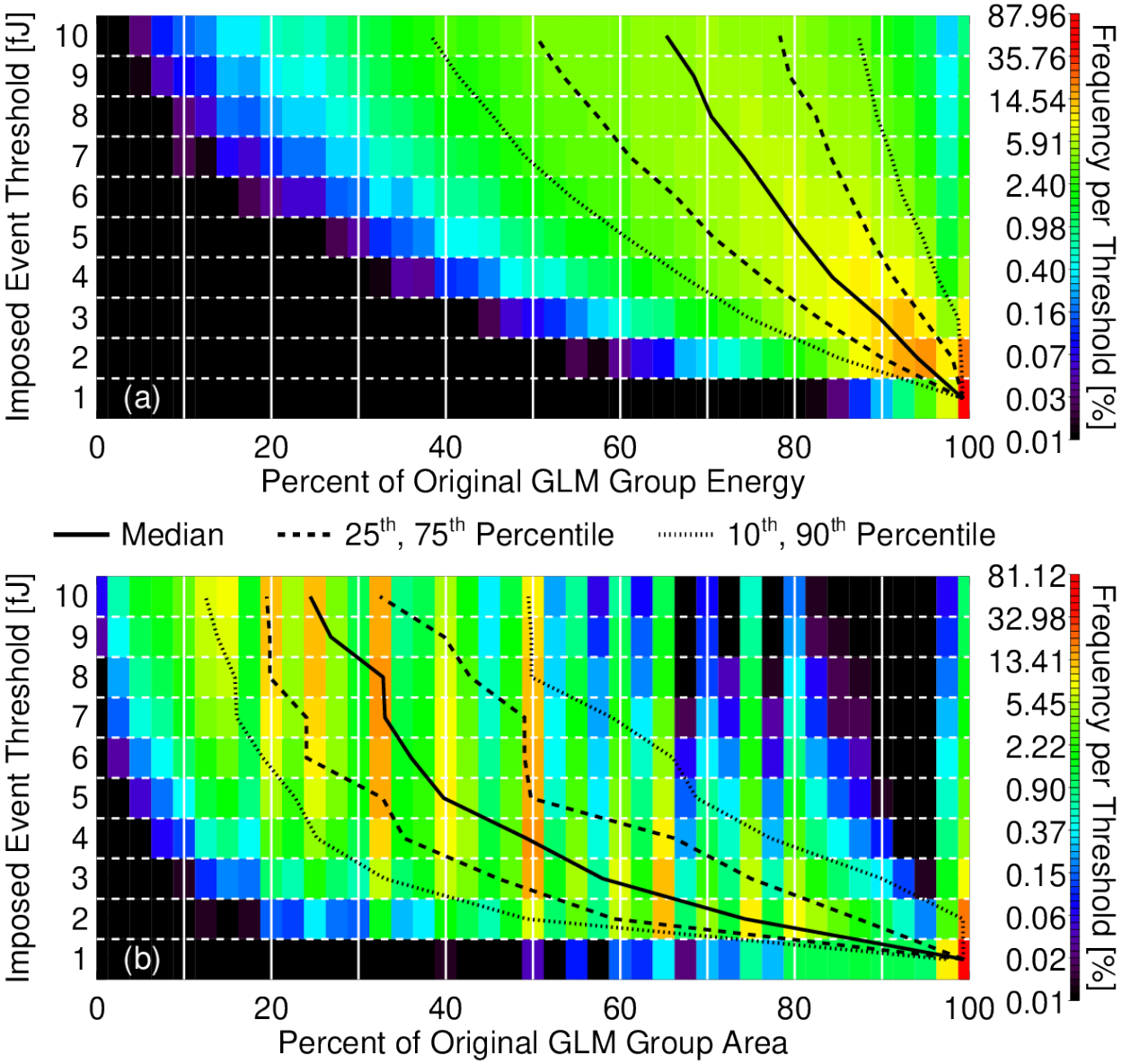

Figure 3. Histograms of GLM (a) group energy and (b) group area under each imposed threshold. Only groups whose maximum event energies exceed 10 fJ are considered.

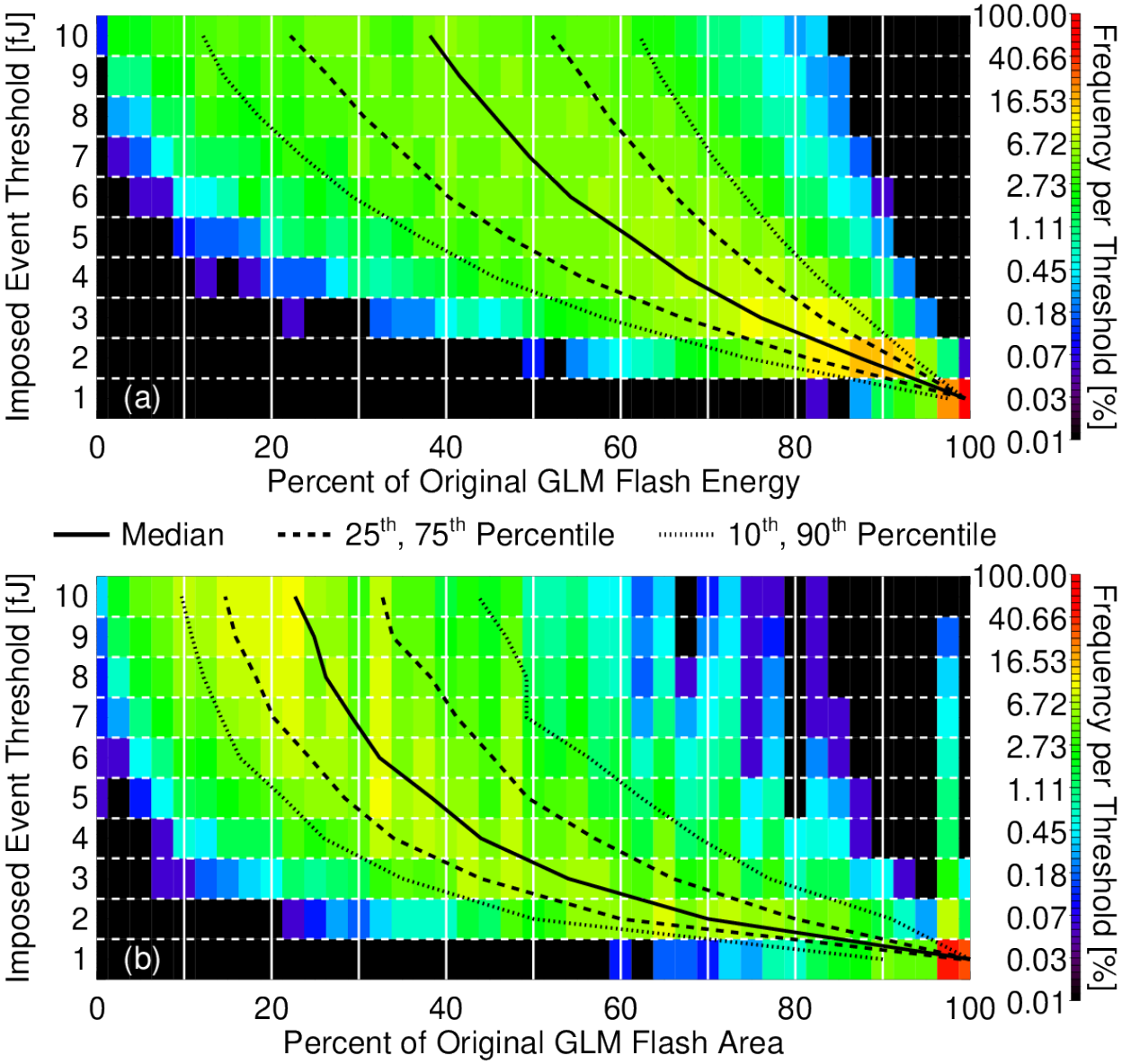

Figure 4. As in Figure 3, but for GLM flashes rather than groups.

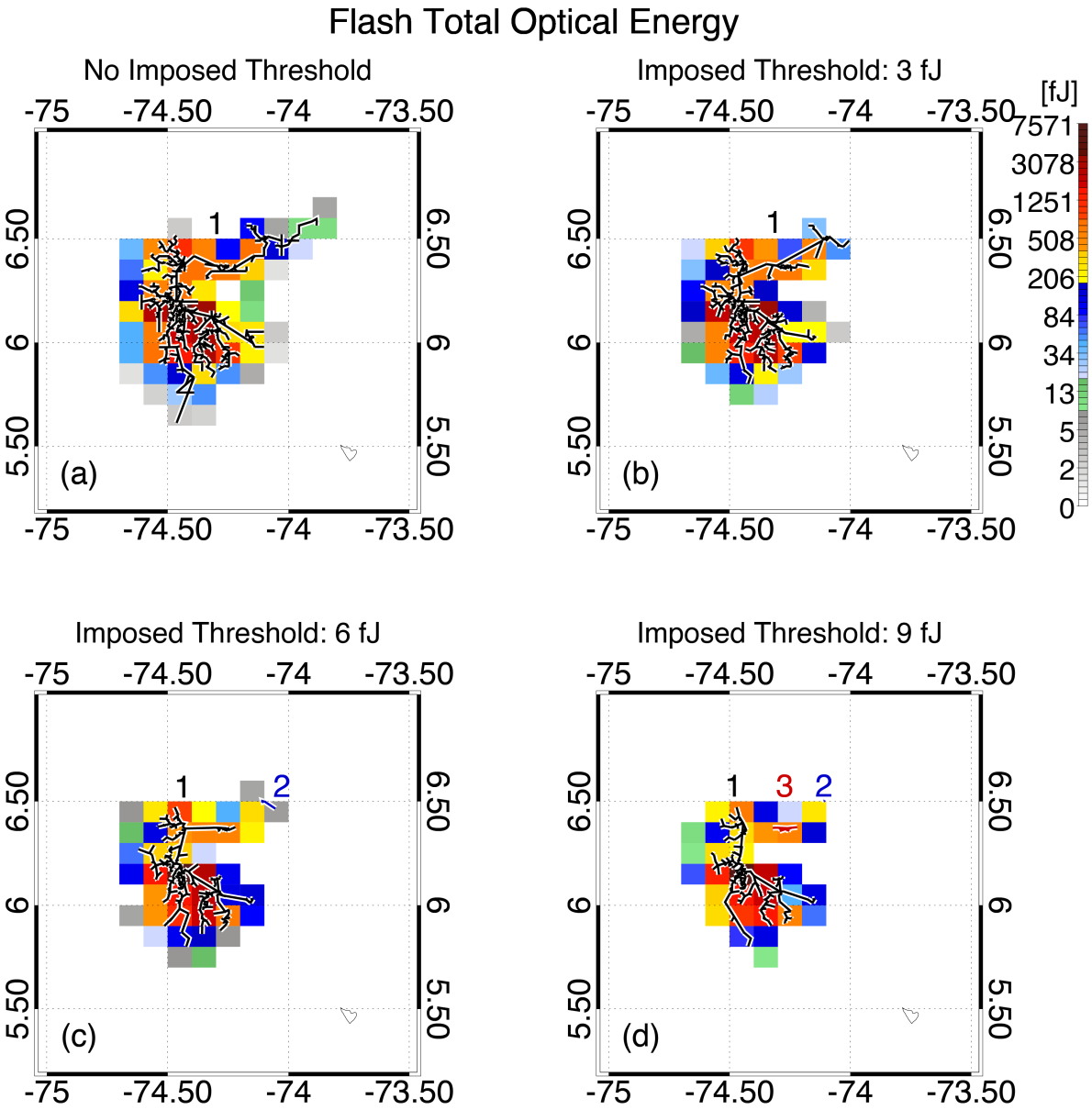

Figure 5. GLM total optical energies (color contour) and progression of groups over time (line segments) from a long horizontal lightning flash under (a) no imposed threshold, (b) a 3 fJ threshold, (c) a 6 fJ threshold, and (d) a 9 fJ threshold. Flash sections that are split at higher thresholds are indicated as disconnected line segments with a unique color and listed index for each split flash.

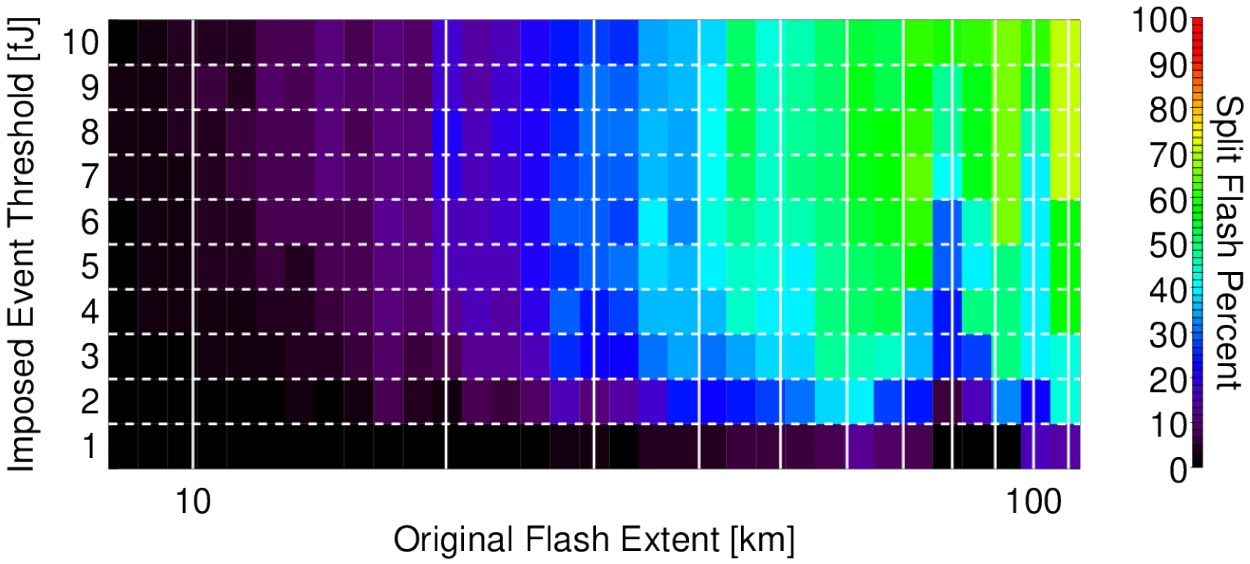

Figure 6. Fractions of flashes that become split after imposing an artificial threshold categorized by original flash extent.

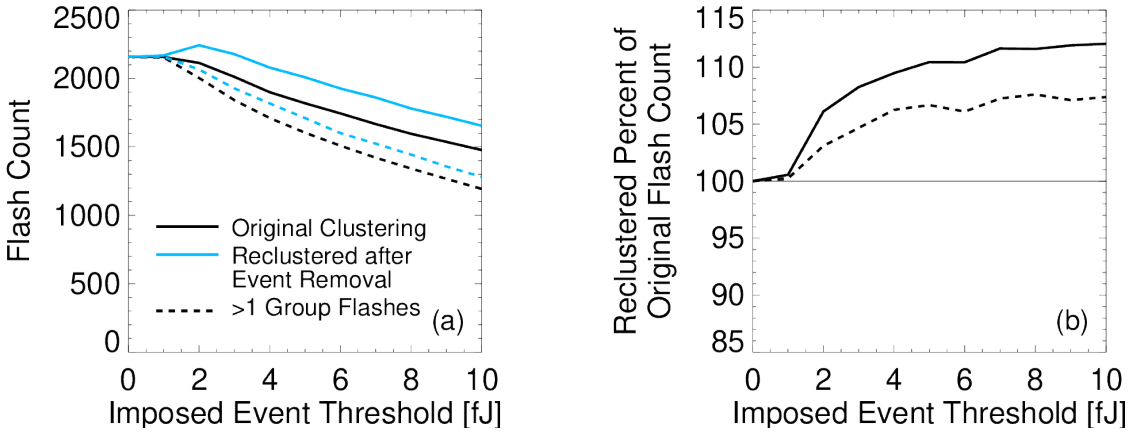

Figure 7. The effect of flash splitting on flash rates. (a) The total number of original flashes (black) and flashes that have been reclustered to account for splitting (blue) at each imposed threshold. (b) The ratio of reclustered flashes to the original flash count at each threshold. Solid lines include all flashes while dashed lines only consider multi-group flashes.

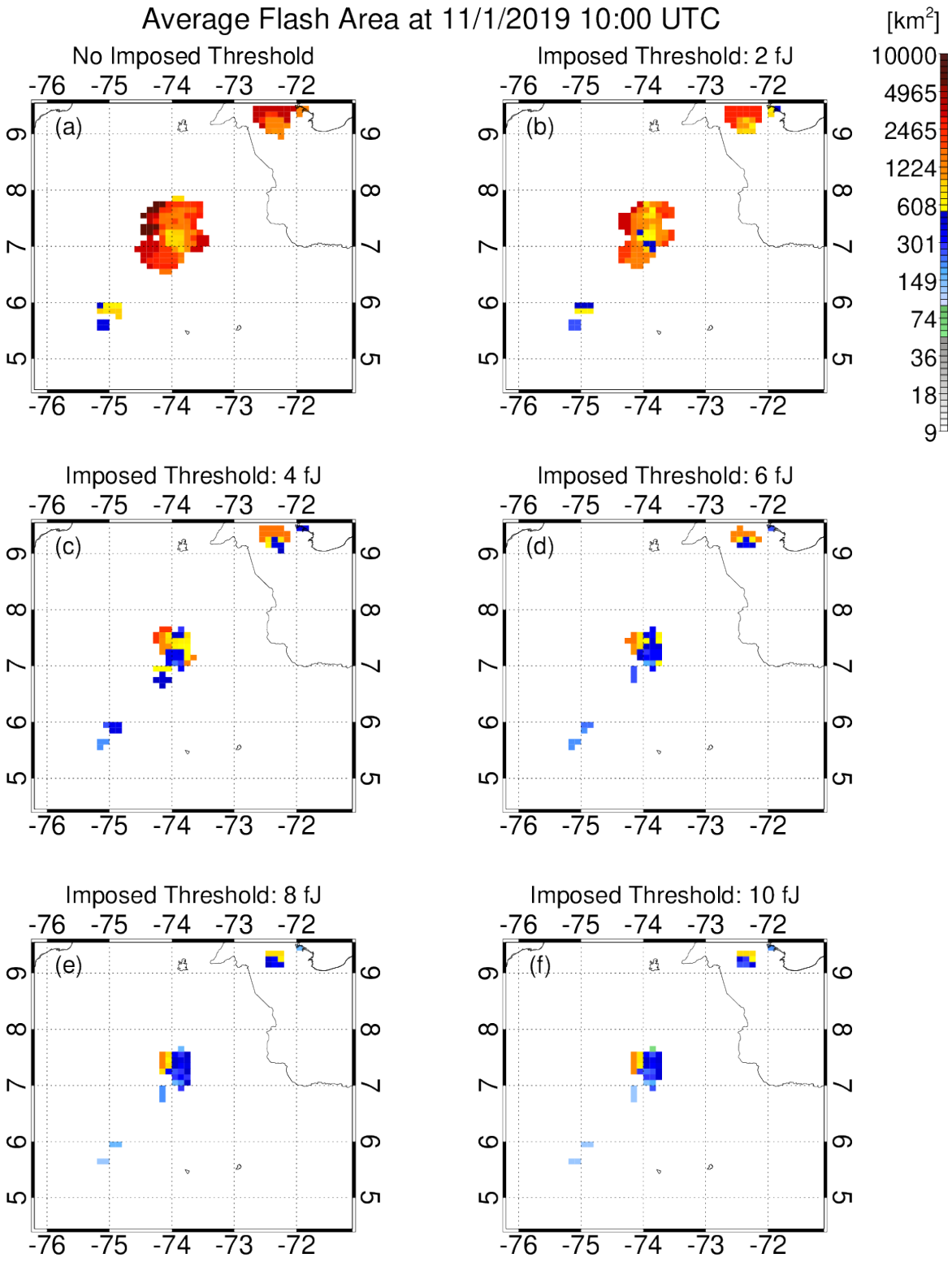

Figure 8. Average Flash Area (AFA) grids generated from (a) the original GLM data and the reclustered data under artificial thresholds of (b) 2 fJ, (c) 4 fJ, (d) 6 fJ, (e) 8 fJ, and (f) 10 fJ.

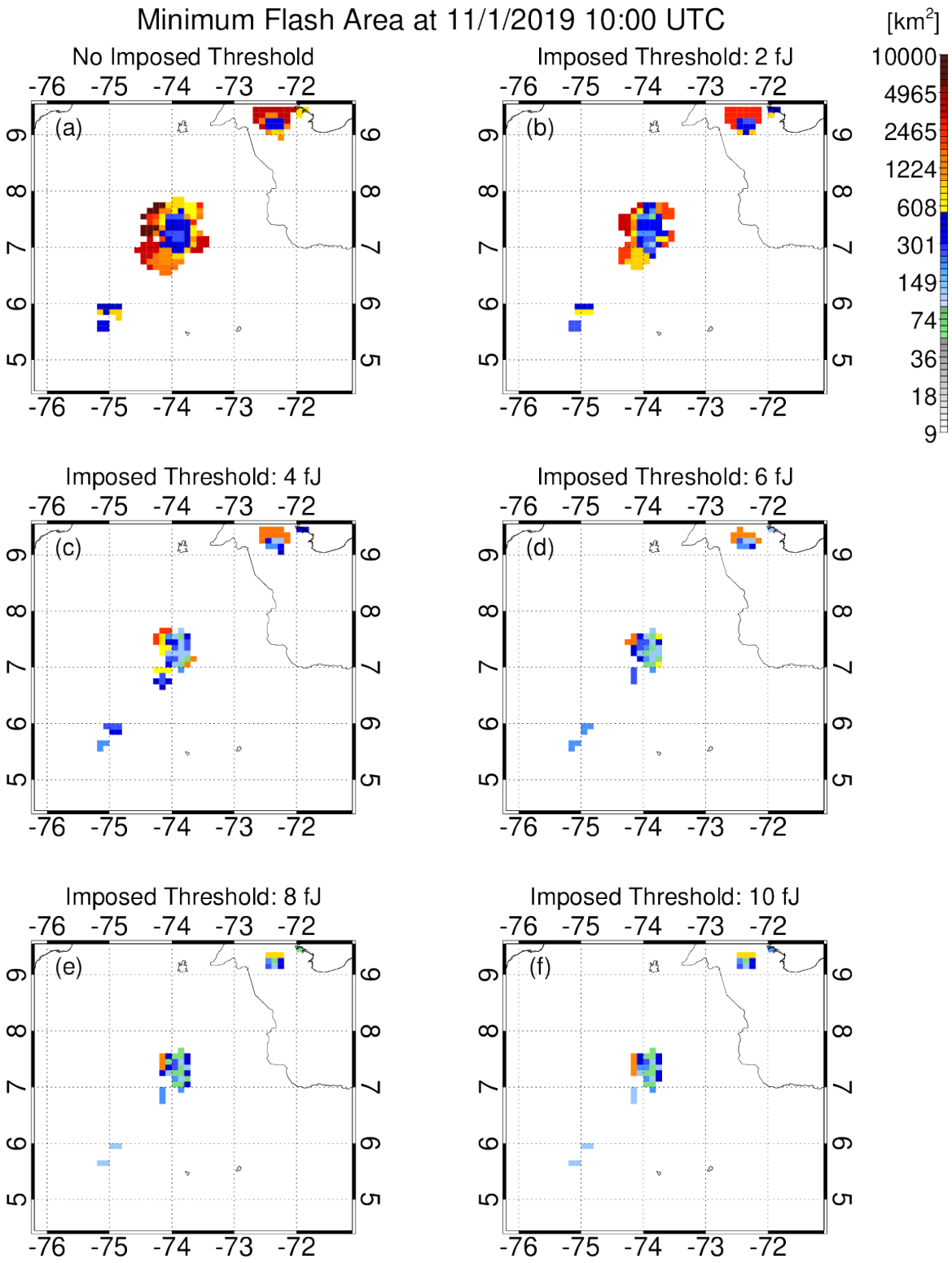

Figure 9. As in Figure 8, but for Minimum Flash Area (MFA) grids.